Dianwei Qian, Shiwen Tong and Xiangjie Liu

Load Frequency Control for Micro Hydro Power Plants by Sliding Mode and Model Order Reduction

Micro hydro is treated as a major renewable energy resource. Such a kind of plants blooms because they can evade some dilemmas like population displacement and environmental problems. But their performance on the frequency index of power systems may be deteriorated in the presence of sudden small load perturbations and parameter uncertainties. To improve the performance, the problem of load frequency control (LFC) raises up. Design of state-based controllers on the aspect of modern control is challenging because only a part of the system states are measurable. This paper addresses the scheme of sliding mode control by model order reduction for the LFC problem of micro hydro power plants. The kind of plants usually has two operating modes, i.e., isolated mode and grid-connected mode. Under each operating mode, mathematical model and model reduction are investigated at first. According to the reduced-order model, a sliding mode control law is subsequently derived. Since the control law is applied to the original system, a sufficient condition about the system stability is proven in light of small gain theory. Simulation results illustrate the feasibility, validity and robustness of the presented scheme.

Key words: Load Frequency Control, Micro Hydro Power Plants, Model Order Reduction, Sliding Mode Control

Upravljanje frekvencijom i radnom snagom mikro hidroelektrana kliznim režimom rada i redukcijom reda modela sustava. Mikro hidroelektrane smatraju se jednim od glavnih obnovljivih izvora energije. Ovakve elektrane su poglavito zanimljive pošto izbjegavaju dileme vezane za iseljavanje ljudi i utjecaj na okoliš. Međutim, njihov učinak na indeks frekvencije energetskih sustava može biti negativan zbog naglih manjih promijena u opterećenju i nesigurnosti parametara. Kako bi se unaprijedila učinkovitost, javlja se problem regulacije frekvencije i radne snage. Projektiranje regulatora po varijablama stanja sustava izazovan je problem, jer je mjerljiv samo dio stanja sustava. Ovaj članak analizira problem upravljanja kliznim režimom rada reducirajući red modela sustava kod regulacije frekvencije i radne snage mikro hidroelektrana. Ovakve elektrane mogu raditi u samostalnom režimu rada ili biti spojene na distribucijsku mrežu. Za oba ražima rada prvo se istražuju matematički modeli te potom njihova redukcija. S obzirom na model reduciranog reda izvodi se upravljački zakon kliznog režima rada. Pošto se zakon upravljanja primjenjuje na izvorni sustav, dokazan je dovoljan uvjet za stabilnost u vidu teorije malog pojačanja. Simulacijski rezutati pokazuju izvedivost, ispravnost i robustnost predloženog pristupa.

Ključne riječi: upravljanje frekvencijom i radnom snagom, mikro hidroelektrane, redukcija reda modela sustava, upravljanje u kliznog režimu rada

1 INTRODUCTION

Micro hydro power is clean, reliable and very efficient in producing electrical energy. Such a kind of renewable energy plays an important role in electrification of rural areas. Usually, micro hydro power plants are more cost-effective and more environment-benign than large hydro power plants, because they can evade some dilemmas like population displacement and environmental problems. Operation of micro hydro power plants is flexible and is deployed in different environments. Usually, there are two operating modes in these plants, i.e., isolated mode and grid-connected mode [1]. Under either mode, consumers

fed by micro hydro power plants require continuous supply of power with good quality. One of the quality indexes is power system frequency. The frequency deviation is inevitable because of an imbalance between generation and load. To maintain the frequency index within permissible limits, a control mechanism entitled load frequency control (LFC) raises up [2, 3].

The LFC problem of micro hydro power plants can be illustrated as a typical disturbance rejection [4]. But its control tasks are subject to variation under different operating modes. The LFC task under the isolated mode is to control the generating electric power in response to the fre-

quency changes within permissible limits. The LFC task under the grid-connected mode is not only to maintain the steady frequency but also to control the net power interchanges in tie line to specified values [5]. Thus, whatever the operating mode is, controller design plays a vital role for the LFC problem of micro hydro power plants [6].

With the property of micro hydro power plants around the world, a variety of control methods for the LFC problem has been reported in the literature, such as fuzzy multi-model control [7], hybrid intelligent control [8], multiple flow control [9], neural-network-based integral control [10], adaptive control [11, 12], to name but a few. A review [13] investigated recent philosophies about operation and control for distribution network connected with small/micro hydro power plants.

Among these presented control methods, sliding mode control (SMC) is attractive due to its invariance property [14–16]. Recently, there has been an increasing interest in applying the control technology [17, 18]. Zargari et al [19] designed a fuzzy sliding-mode governor to solve the frequency control problem of an isolated small hydropower system. In [20, 21], two kinds of sliding-mode governors were investigated for hydropower plants. Other reports can be found in [22–24]. Usually, one assumption in most of the referred articles is that all the state variables of hydro power systems are measurable. In practice, only a part of states are measurable so that it is desired to have the minimum number of state variables for the LFC controller design of micro hydro power systems.

This paper focuses on the topic and addresses the scheme of the model-reduction-based SMC for the LFC problem of micro hydro power plants. Since micro hydro power plants have both isolated and grid-connected operating modes, dynamics model of each component under the two modes is described at first. Under each operating mode, the method of model order reduction is employed to simplify the system by analyzing the models. A SMC-based controller is designed according to the reduced-order LFC system model. To guarantee the controller can stabilize the original LFC system, a sufficient condition is drawn from small gain theorem. Simulation results illustrate the feasibility, validity and robustness of the presented control approach.

2   SYSTEM DYNAMICS

Modelling the LFC problem of micro hydropower plants depends on operating modes. Whatever the operating mode is, some basic components are included, i.e., turbine & its feeding penstock, valve & its servomotor, generator & power system. Block diagrams under the two operating mode are illustrated in Fig. 1, where Fig. 1(a) indicates the isolated mode and Fig. 1(b) means the grid-connected mode with the assumption of infinite bus.

In Fig. 1, the LFC control task under the grid-connected mode is with a relatively difficulty because one more component, tie line, complements. The task is met by measuring an error signal, called area control error (ACE), which represents the power imbalance between generation and load. Transfer functions of these components can be drawn from small signal analysis because the control problem under consideration is in the presence of relatively small changes. The component models are presented in [8] and [25].

1) Turbine & penstock: The approximate transfer function of the turbine and penstock component for the analyses in [8] is given as

$$G_t(s) = \frac{\Delta P_G(s)}{\Delta X(s)} = \frac{-T_w s + 1}{\frac{T_w}{2} s + 1} \tag{1}$$

here T_w (s) is nominal starting time of water in penstock, s is Laplace transform complex variable operator, ΔP_G (per unit) is incremental power (torque) output of turbine, ΔX (per unit) is incremental power input to the turbine (valve position). Note that water flow in the penstock is subject to the phenomenon of water hammer, which result in a non-minimum phase system (1). Further, the water-hammer effect means an initial tendency exists for the torque changes in an opposite direction to the water-flow changes.

2) Valve & servomotor: Usually, a DC servomotor with closed-loop armature control is employed to regulate the water flow rate in the penstock. The flow of water is regulated by controlling the valve position. The transfer function of the mechanical and electrical component in [8] is displayed as

$$G_V(s) = \frac{1}{T_e s + 1} \frac{1}{T_m s + 1} \tag{2}$$

here T_m (s) is mechanical time constant, T_e (s) is electrical time constant. In addition, unity gain is applied as a feedback to depict the closed-loop armature control of this DC servomotor. At last, the transfer function of this component is given as

$$\frac{\Delta X(s)}{\Delta P_c(s) - \frac{1}{R} \Delta F(s)} = \frac{G_V(s)}{1 + G_V(s)} \tag{3}$$

here R (Hz/p.u.kW) is a constant of steady state speed regulation, ΔX (per unit) is gate position deviation, ΔF (Hz) is frequency deviation, ΔP_c (per unit kW) is incremental speed changer position.

3) Generator & power system: According to the load-frequency characteristic, a load damping term is employed to describe the swing equation of a synchronous generator
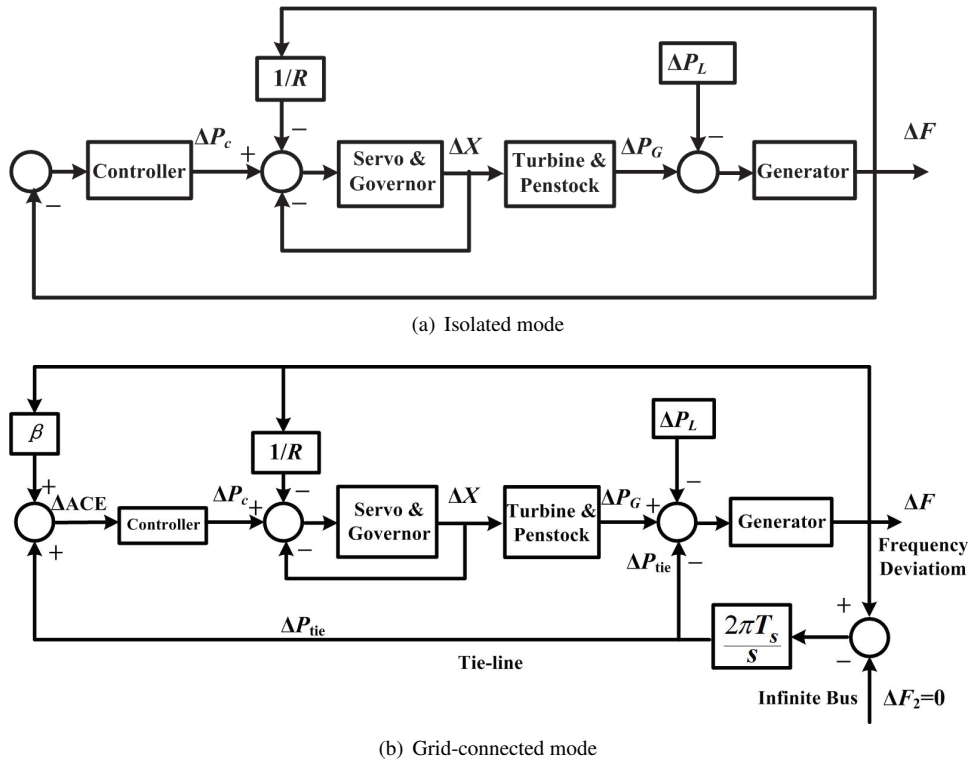
(a) Isolated mode

(b) Grid-connected mode

Fig. 1. Block diagrams under the two operatating modes

[25]. By taking Laplace transform for the equation, the generator dynamics is able to be gotten as

$$G_P(s) = \frac{\Delta F(s)}{\Delta P_G(s) - \Delta P_L(s)} = \frac{K_p}{T_p s + 1} \qquad (4)$$

here ΔP_L (per unit kW) is step function load disturbance, K_p is generator gain constant, defined by $K_p = \frac{1}{D} = 1/\frac{\partial P_L}{\partial F}$, T_P (s) is generator time constant, defined by $T_p = \frac{2H}{f^0 D}$, where H is inertia constant of synchronous generator, f^0 (Hz) is nominal system frequency.

4) Tie line: A transmission line that joins two power systems together is entitled as tie line. Obviously, there is no tie line under the isolated mode. The incremental power change in the tie line [25] is depicted as

$$\Delta P_{tie}(t) = 2\pi T_s \int \Delta F(t) \mathrm{d}t \qquad (5)$$

here T_s (p.u.kW/rad) is synchronizing power coefficient of tie line , ΔP_{tie} (per unit kW) is the power flow in the tie line from the generator to the grid system. By taking Laplace transfer, the above equation can be transformed as

$$G_{tie}(s) = \frac{\Delta P_{tie}(s)}{\Delta F(s)} = \frac{2\pi T_s}{s} \qquad (6)$$

5) ACE: under the grid-connected mode, not only should the frequency of each control area return to its nominal value, but also the net power interchange through the tie line should return to the scheduled values. To achieve the composite goal, ACE in (7) is defined by a linear combination of power interchange and frequency deviations.

$$\Delta ACE = \beta \Delta F + \Delta P_{tie} \qquad (7)$$

here β (p.u.kW/Hz) is the frequency bias factor of this area.

3 CONTROL DESIGN & STABILITY ANALYSIS

3.1 Model Analysis and Order Reduction

With the development of sensor and measuring technology, many methods have been proposed to obtain internal information from an industrial process. This extends the ability of control design. Most of the mentioned state-based LFC controllers of micro hydro power plants [1, 2, 6–13, 19] usually have an assumption that all the system states are measurable. The assumption is too strict to be achieved in practice. In Fig. 1, it can be found that the following three independent state variables, i.e., ΔP_G, ΔX and ΔF, are directly measurable and available for the LFC controller design. Compared with the system models in Section 2, the one-order dynamics (1) can be depicted by the state variable ΔP_G and (4) can be described

by ΔF. But (3) is a two-order dynamics with only one measurable and independent state variable ΔX. In a word, order of the valve and servo component should be reduced because the number of its measurable state variable is less than its system order.

The dynamic equation in (2) consists of two terms. Note that the electrical time constant T_e is usually 10 times smaller than the mechanical time constant T_m. According to the method of model order reduction [26], (2) can be simplified by

$$G_{SV}(s) = \frac{1}{(T_e + T_m)s + 1} \qquad (8)$$

Compared with (2), (8) is a one-order dynamic equation and the measurable and independent state variable ΔX can depict it. It is necessary to check the accuracy of the simplified model (8) in frequency domain. Provided $T_e = 0.01$ s and $T_m = 0.001$ s (given in [8]), comparison of the frequency response curves is shown in Fig. 2, where the blue solid line means the original system and the green solid line means the simplified one.

Fig. 2 shows the two plots are almost the same as each other at low frequencies. This case means the simplified system is able to depict the dynamics of the original one if the system is at low frequencies. Fortunately, the condition is usually satisfied because the load disturbance ΔP_L is always step signal so that the simplified system is accurate enough to be adopted for control design for rejecting the step load disturbance ΔP_L.
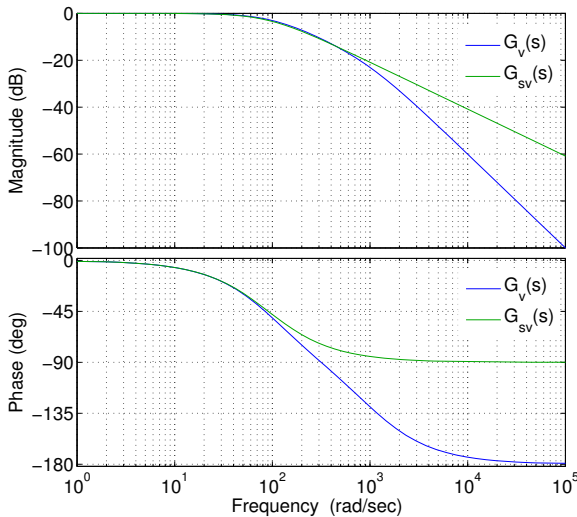

Fig. 2. Frequency response curves

3.2 Isolated Mode

The block diagram in Fig. 3 shows an isolated power system fed by micro hydropower plants. Fig. 3 illustrates

blue lines are measurable state variables for the control design. According to the control task under the isolated operating mode, the frequency deviation ΔF is the exclusive state variable to be regulated. To eliminate the frequency deviation, the integral of ΔF with a known gain K_E^i is defined as an additional state x_{add}^i [27, 28].

$$x_{add}^i(t) = K_E^i \int_0^\infty \Delta F(t)\mathrm{d}t \qquad (9)$$

With the additional state, the state expression to depict the reduced-order system drawn from the block diagram Fig. 3 able to be written as

$$\begin{aligned} \dot{\mathbf{x}}_i &= \mathbb{A}_i\mathbf{x}_i + \mathbb{B}_i u + \mathbb{F}_i d_i(t) \\ y_i &= \mathbb{C}_i^T\mathbf{x}_i \end{aligned} \qquad (10)$$

here $\mathbf{x}_i = [\Delta F(t), \Delta P_G(t), \Delta X(t), x_{add}^i(t)]^T$ is state vector, $d_i(t)$ is disturbance signal, $u_i(t) = \Delta P_c$ is control input. State matrix $\mathbb{A}_i$, input vector $\mathbb{B}_i$, output vector $\mathbb{C}_i$ and disturbance vector $\mathbb{F}_i$ are shown in Appendix.

To design the reduced-order sliding mode LFC controller, the sliding surface variable S_i should be defined at first.

$$S_i = \mathbf{c}_i^T\mathbf{x}_i \qquad (11)$$

here $\mathbf{c}_i$ is constant and it is with the same dimension as $\mathbf{x}_i$. According to the SMC methodology, a SMC law consists of equivalent control law and switching control law [14–16]. The equivalent control law ensures the system trajectory stays on the surface after reaching the sliding mode. The switching control law is usually designed as a sign function related to the sliding surface variable and it can guarantee the control system is of asymptotical stabilization. Thus, the control law u_i is defined as

$$u_i = u_{ieq} + u_{isw} \qquad (12)$$

Here u_{isw} is the switching control and u_{ieq} is the equivalent control law. The expressions of u_{isw} and u_{ieq} will be deduced below.

When the system states keep sliding on the surface (11), only the equivalent control u_{ieq} works [14]. Differentiating S_i with respect to time t yields

$$\dot{S}_i = \mathbf{c}_i^T\dot{\mathbf{x}}_i = \mathbf{c}_i^T(\mathbb{A}_i\mathbf{x}_i + \mathbb{B}_i u_{ieq}) = 0 \qquad (13)$$

Substituting the nominal system of (10) into (13) yields

$$u_{ieq} = -(\mathbf{c}_i^T\mathbb{B}_i)^{-1}\mathbf{c}_i^T\mathbb{A}_i\mathbf{x}_i \qquad (14)$$

To guarantee the control law (12) makes the sliding-surface variable S_i asymptotically stable, a Lyapunov function is selected as
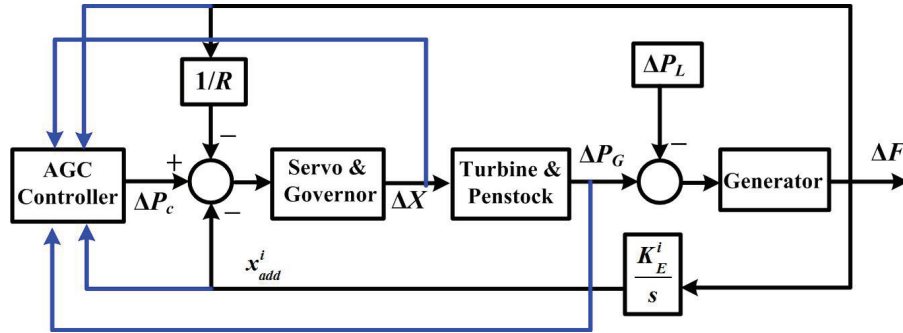
$$V_i(t) = \frac{1}{2}S_i^2 \qquad (15)$$

Fig. 3. Block diagram with an additional state under the isolated mode.

Differentiating V_i with respect to time t and substituting (10)–(12) and (14) into it obtain

$$
\begin{aligned}
\frac{\mathrm{d}V_i}{\mathrm{d}t} &= S_i \dot{S}_i = S[\mathbf{c}_i^T \dot{\mathbf{x}}_i] \\
&= S_i \mathbf{c}_i^T [\mathbb{A}_i \mathbf{x}_i + \mathbb{B}_i u + \mathbb{F}_i d_i(t)] \\
&= S_i \mathbf{c}_i^T [\mathbb{A}_i \mathbf{x}_i + \mathbb{B}_i (u_{ieq} + u_{isw}) + \mathbb{F}_i d_i(t)] \\
&= S_i [\mathbf{c}_i^T (\mathbb{A}_i \mathbf{x}_i + \mathbb{B}_i u_{ieq}) + \mathbf{c}_i^T \mathbb{B}_i u_{isw} + \mathbf{c}_i^T \mathbb{F}_i d_i(t)] \\
&= S_i [\mathbf{c}_i^T \mathbb{B}_i u_{isw} + \mathbf{c}_i^T \mathbb{F}_i d_i(t)]
\end{aligned}
$$
(16)

Let $\mathbf{c}_i^T \mathbb{B}_i u_{isw} = -\kappa_i S_i - \eta_i sgn(S_i)$ where κ_i and η_i are positive constants, $\eta_i \geq \| \mathbf{c}_i^T \mathbb{F}_i d_i(t) \|_\infty$ and $sgn(\cdot)$ is sign function. Then, the switching control law u_{isw} is obtained as

$$ u_{isw} = -(\mathbf{c}_i^T \mathbb{B}_i)^{-1}[\kappa_i S_i + \eta_i sgn(S_i)] \qquad (17) $$

Finally, the SMC law under the isolated mode can be gotten as

$$ u_i = -(\mathbf{c}_i^T \mathbb{B}_i)^{-1}[\mathbf{c}_i^T \mathbb{A}_i \mathbf{x}_i + \kappa_i S_i + \eta_i sgn(S_i)] \quad (18) $$

Note that u_i in (18) is deduced from the system dynamics in the form of reduced order. But (18) will be applied to the original dynamics without order reduction in the following simulations. Consequently, it is necessary to analyze whether the SMC controller based on the reduced-order dynamics is able to stabilize the original system or not. In [26], Saxena and Hote employed a reduced-order model and presented an internal model controller for the LFC of power systems. But they did not investigate such a theoretical analysis.

Theorem 1 *If (19) is satisfied, then the control law (18) is able to stabilize the original system.* □

$$ \| \Delta \|_\infty \leq \| \frac{1}{G_0(s)+1} \|_\infty + \| G_{SV}(s) \|_\infty \qquad (19) $$

where $G_0(s) = G_t(s)G_P(s)(\frac{K_E^i}{s} + \frac{1}{R})$.

Proof: Define $\Delta = G_V(s) - G_{SV}(s)$ as error between $G_V(s)$ and $G_{SV}(s)$, then the block diagram in Fig. 4(a) under the isolated mode is able to be drawn from Fig. 3. The block in Fig. 4(a) can be simplified by block diagram algebra. The process is illustrated in Fig. 4(b), where $\delta = \frac{\Delta}{G_{SV}(s)}$ and $G(s) = -G_{SV}(s)[G_0(s)+1]$.

From the design process, the sliding-mode LFC controller can asymptotically stabilize the reduced order system so that $\frac{G(s)}{1-G(s)}$ is of input-output stability with respect to the input ε_1 and the output ε_2 in Fig. 4(b). Consequently, (20) can be obtained in the frequency domain.

$$
\begin{aligned}
\varepsilon_2 &= W(s)\varepsilon_1 \\
\varepsilon_1 &= \delta(s)\varepsilon_2
\end{aligned}
\qquad (20)
$$

where $W(s) = \frac{G(s)}{1-G(s)}$. Note that the last diagram in Fig. 4(b) is just the general framework for robust stability analysis of interconnected systems [29]. On account of small gain theorem [29], a sufficient condition for stabilizing the original system in Fig. 3 is obtained as

$$ \| \delta(s) \cdot W(s) \|_\infty \leq 1 \qquad (21) $$

i.e., $\| \Delta \|_\infty \leq \| \frac{G_{SV}(s)G_0(s) + G_{SV}+1}{G_0(s)+1} \|_\infty$.

From (21), we have $\| \Delta \|_\infty \leq \| G_{SV}(s) + \frac{1}{G_0(s)+1} \|_\infty$. In light of the Cauchy-Schwarz inequality, the sufficient condition (19) can be drawn. ∎

3.3 Grid-connected Mode

The block diagram in Fig. 5 illustrates a power system (control area) connected to an infinite bus. Shown in Fig. 5, the power system under the grid-connected mode is not only fed by micro hydro power plants, but also is supported by other sources via the tie line. Fig. 5 also illustrates blue lines depict measurable state variables for the control design.

In Fig. 5, the bus is infinite so that its frequency F_2 is kept as a constant. The deviation of F_2, ΔF_2, is set as

(a) Block diagram of the simplified system with error under the isolated mode.

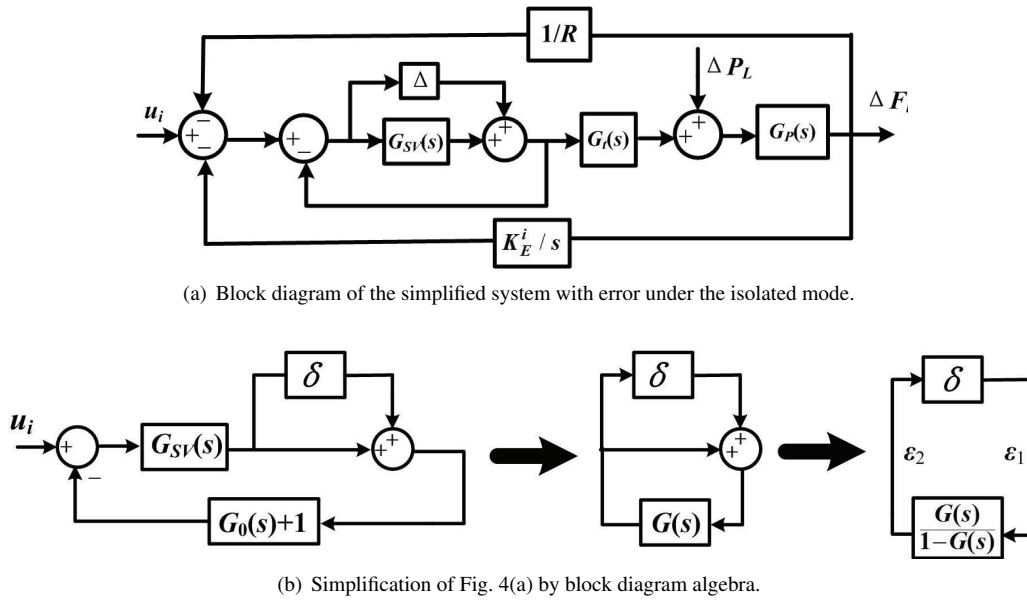(b) Simplification of Fig. 4(a) by block diagram algebra.

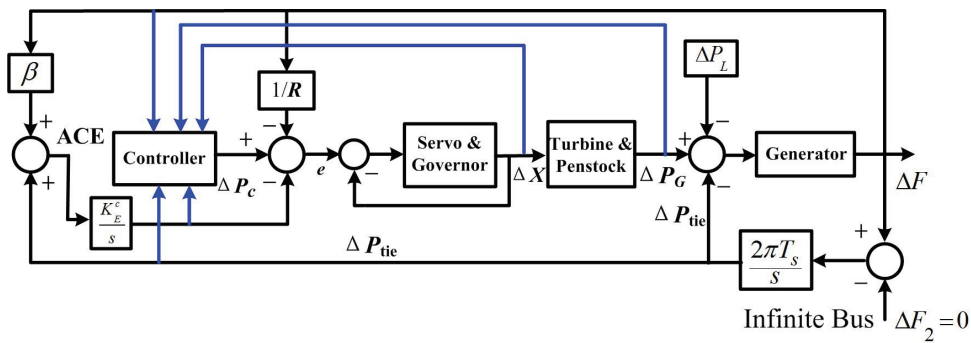*Fig. 4. Stability analysis under the isolated mode*

Fig. 5. Block diagram with an additional state under the grid-connected mode.

zero because the considered LFC problem is in presence of relatively small changes. The control object under the mode contains two parts. One is to eliminate the frequency deviation in the control area. The other is to keep the net power from the tie line zeroth. To simultaneously achieve the two parts, the ACE measure in (7) is introduced. To realize the zeroth ACE, the integral of ΔACE with a known gain K_E^c, is defined as an additional state [30].

$$x_{add}^c(t) = K_E^c \int_0^\infty \Delta ACE \, \mathrm{d}t \qquad (22)$$

The model reduction process is similar to the design under the isolated mode. Dynamics of the reduced-order system can be described as

$$\begin{aligned} \dot{\mathbf{x}}_c &= \mathbb{A}_c \mathbf{x}_c + \mathbb{B}_c u_c + \mathbb{F}_c d_c(t) \\ y_c &= \mathbb{C}_c^T \mathbf{x}_c \end{aligned} \qquad (23)$$

here $\mathbf{x}_c = [\Delta F(t), \Delta P_G(t), \Delta X(t), \Delta P_{tie}(t), x_{add}^c(t)]^T$ is defined as state vector, $d_c(t) = \Delta P_L$ is disturbance signal and $u_c = \Delta P_c$ is control input. State matrix $\mathbb{A}_c$, input vector $\mathbb{B}_c$, output vector $\mathbb{C}_c$ and disturbance vector $\mathbb{F}_c$ are shown in Appendix.

Define the sliding surface $S_c = \mathbf{c}_c^T \mathbf{x}_c$ where $\mathbf{c}_c$ is constant and it is with the same dimension as $\mathbf{x}_c$. By adopting the equivalent control plus switching control method, the control law can be derived as

$$u_c = -(\mathbf{c}_c^T \mathbb{B}_c)^{-1}[\mathbf{c}_c^T \mathbb{A}_c \mathbf{x}_c + \kappa_c S_c + \eta_c sgn(S_c)] \quad (24)$$

where $sgn(\cdot)$ is sign function, κ_c and η_c are positive constants, and $\eta_c \geq \parallel \mathbf{c}_c^T \mathbb{F}_c d_c(t) \parallel_\infty$. The process of control design is also similar to the design under the isolated mode. Similarly, it is necessary to analyze whether the SMC controller based on the reduced-order dynamics is able to stabilize the original system or not.
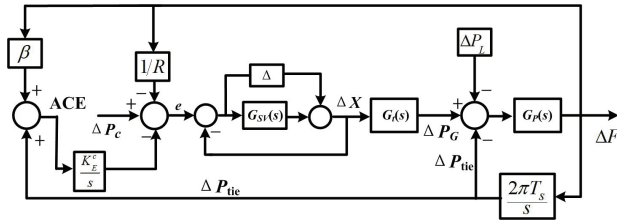
(a) Block diagram of the simplified system with error under the grid-connected mode.
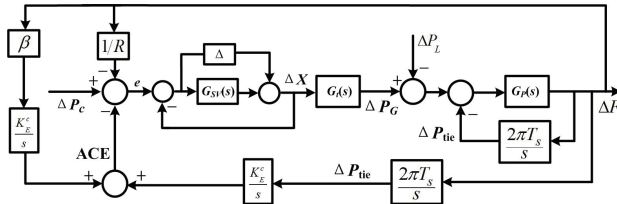
(b) Simplification of each branch in Fig. 6(a) by block diagram algebra.
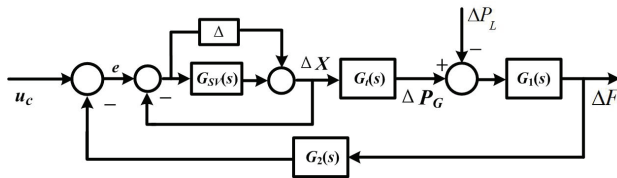
(c) Mergence of all the branches in Fig. 6(b) by block diagram algebra.

Fig. 6. Simplification of the block diagram by block diagram algebra under the grid-connected mode.

Theorem 2 *If (25) is satisfied, then the control law (24) is able to stabilize the original system.* □

$$\| \Delta \|_\infty \leq \| \frac{1}{G_1(s)G_2(s)G_t(s)+1} \|_\infty + \| G_{SV}(s) \|_\infty \tag{25}$$

where $G_1(s) = \frac{sG_P(s)}{s+2\pi T_s G_P(s)}$ *and* $G_2(s) = \frac{2\pi T_s K_E^c}{s^2} + \frac{\beta K_E^c}{s} + \frac{1}{R}.$

Proof: Define $\Delta = G_V(s) - G_{SV}(s)$ as error between $G_V(s)$ and $G_{SV}(s)$, then the block diagram in Fig. 6(a) under the grid-connected mode is able to be drawn from Fig. 5.

The block in Fig. 6(a) can be simplified by block diagram algebra. Define $\delta = \frac{\Delta}{G_{SV}(s)}$, $G_1(s) = \frac{sG_P(s)}{s+2\pi T_s G_P(s)}$, $G_2(s) = \frac{2\pi T_s K_E^c}{s^2} + \frac{\beta K_E^c}{s} + \frac{1}{R}$ and $G_3(s) = -G_{SV}(s)[1 + G_1(s)G_2(s)G_t(s)]$, the the simplification process is illustrated in Fig. 6(b), 6(c), and Fig. 7.

From the design process, the sliding-mode LFC controller can asymptotically stabilize the reduced order system under the grid-connected mode so that $\frac{G_3(s)}{1-G_3(s)}$ is of input-output stability with respect to the input ε_3 and the output ε_4 in Fig. 7. Finally, (26) can be obtained in the

frequency domain.

$$\varepsilon_4(s) = \frac{G_3(s)}{1 - G_3(s)}\varepsilon_3(s)$$
$$\varepsilon_3(s) = \delta(s)\varepsilon_4(s) \tag{26}$$

Note that the last diagram in Fig. 7 is just the general framework for robust stability analysis of interconnected systems [29]. On account of small gain theorem [29], a sufficient condition for stabilizing the original system in Fig. 5 can be obtained as

$$\| \delta(s) \cdot \frac{G_3(s)}{1 - G_3(s)} \|_\infty \leq 1 \tag{27}$$

i.e., $\| \Delta \|_\infty \leq \| \frac{G_{SV}(s)G_1(s)G_2(s)G_t(s)+G_{SV}(s)+1}{G_1(s)G_2(s)G_t(s)+1} \|_\infty.$

$\| \Delta \|_\infty \leq \| G_{SV}(s) + \frac{1}{G_1(s)G_2(s)G_t(s)+1} \|_\infty$ can be derived from (27). Finally, (25) can be obtained according to the Cauchy-Schwarz inequality. ■

Remark: The two sliding mode controllers (18) and (24) are designed on the reduced-order models (10) and (23), respectively. Consequently, the sliding modes only exist in the reduced-order models, rather than the original models. In other words, here the SMC methodology is just employed as a design tool and there is no guaranteed sliding modes in the control systems for the original models. However, the controllers based on the reduced order models cannot theoretically guarantee the system stabilities for the original systems. To attack the issue, Theorems 1 and 2 investigate this field and archive the inequalities between the reduced-order error and the systems stabilities.

4 SIMULATIONS

In this section, typical parameters of a micro hydro power system are considered in the following simulations. The data in [8] are taken as benchmarks. Total rated capacity of the generation unit is 50 kW, normal operating load is 25 kW, regulation coefficient R is 10 Hz/pu·kW. Provided that load-frequency dependency is linear, nominal load is 48% of the rated load and ΔP_L=3%. The nominal starting time of water in penstock T_w is 4 s. The generator parameters are determined as K_p=50 Hz/pu·kW and T_p =64.64 s. The governor & servo coefficients are kept as T_e = 0.01 s and T_m = 0.001 s.

4.1 Isolated Mode

Under the isolated mode, the micro hydro unit serves as an exclusive source to feed the area. No other source is able to be adopted to regulate the frequency in the area. The frequency in the isolated area is an exclusive objective to be regulated. The sliding surface parameters in (10)
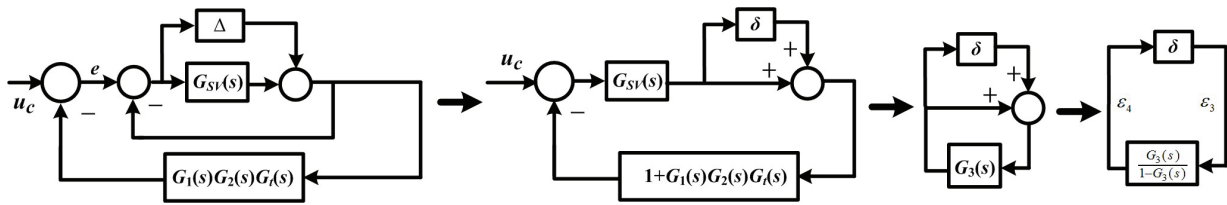
Fig. 7. Stability analysis under the grid-connected mode.

are selected as $\mathbf{c}_i = [9.0\ 2.0\ 6.0\ 0.1]^T$ according to Ackermann's formula. Gain of the additional state is 0.002. Other controller parameters in (18) are picked up as $\kappa_i = 1$ and $\eta_i = 0.01$. The load disturbance $\Delta P_L = 3\%$ is applied to the system at $t = 0$.

As shown in Fig. 8, the blue plots are the results by a PID controller tuned by internal model control (IMC) [26] and [31]. The output of this PID controller is determined by $u_{PID}(s) = (K_p^{IMC} + \frac{K_i^{IMC}}{s} + sK_d^{IMC})\Delta F(s)$, the parameters of which are $K_p^{IMC} = 0.056$, $K_i^{IMC} = 0.002$ and $K_d^{IMC} = 0.0001$. Compared with the results by the IMC-PID controller, the frequency-deviation curve by the designed sliding mode LFC controller has smaller overshooting and shorter settling time. The curves by the designed controller have larger overshooting on the aspects of ΔP_G and ΔX, but these cases indicate that the designed controller can open the valve and increase the turbine output the moment that the load disturbance ΔP_L injects the system, rather than the IMC-PID control system with a slow response. Thus, the designed controller has better performance in the presence of load disturbances.

4.2 Grid-connected Mode

Under the grid-connected mode, the control area is not only fed by the micro hydro power unit, but also is supported by the source from an infinite bus by tie line. Thus, the control object under this mode contains two parts. One is to eliminate the frequency deviation in the control area. The other is to keep the net power from the tie line zeroth. To realize the composite object, we introduce the ACE measure. In this subsection, parameter of the ACE variable β is 0.2083 p.u.kW/Hz [25], synchronizing power coefficient of the tie line T_s is 0.0866 s [25], gain of the additional state is picked up as 0.002. The sliding surface parameters of the SMC controller in (24) are selected as $\mathbf{c}_c = 10^8 \cdot [0.0001\ 0.0007\ 0.0014\ 0.0001\ 2.4337]^T$ according to Ackermann's formula. Other controller parameters in (24) are picked up as $\kappa_c = 0.1$ and $\eta_c = 0.1$. The load disturbance ΔP_L is applied to the system at $t = 0$.

In Fig. 9, the blue plots are the results by an IMC-PID controller. The output of the PID controller is determined by $u_{PID}(s) = (K_p^{IMC} + \frac{K_i^{IMC}}{s} + sK_d^{IMC})\Delta ACE(s)$, the

parameters of which are selected as $K_p^{IMC} = 0.66$, $K_i^{IMC} = 0.06$ and $K_d^{IMC} = 0.001$. Illustrated in Fig. 9, both the IMC-PID controller and the SMC controller can eliminate the frequency deviation and the area control error, simultaneity keep the net power of the time line zeroth. Both of them are able to realize the control object of the grid-connected mode. From the plot of ΔF, the designed controller, compared with the IMC-PID controller, is with faster response to the load disturbance ΔP_L although it is indeed with a larger overshooting. On the other hand, the plot by the IMC-PID controller is damped oscillation with 5 times, while the design controller can stabilize the system frequency with only once oscillation.

Compared with the curves of ΔF and ΔP_{tie}, the frequency deviation in the control area is very quickly eliminated in 10 s, but it takes about 40 s to eliminate the power deviation in tie line, ΔP_{tie}. This indicates the frequency in the control area under the grid-connected mode is with the better performance because the area is also fed by the infinite bus from the tie line, but it takes more time for the entire interconnected electric power system to eliminate the power deviation in the tie line for keeping a zeroth ΔP_{tie}.

Moreover, compared with Figs. 8 and 9, it is obvious the dynamic process of the frequency deviation ΔF in Fig. 9 has a smaller settling time under the same load disturbance $\Delta P_L = 3\%$. The reason of the phenomena is explained as follow. Under the isolated mode, the control area is only fed by the exclusive micro hydro power plant and the system frequency is regulated by the LFC controller. A long settling time is necessary for the system to increase the power output ΔP_G for resisting the load disturbance ΔP_L. Under the grid-connected mode, the control area is simultaneously fed by the plant and the tie line. When there is a load disturbance, the tie line can support the control area to resist the disturbance by absorbing power from the infinite bus, meanwhile, the plant also increases its power output to feed on the control area. This process makes the settling time under the grid-connected mode much smaller. This is also a benefit we can earn from interconnected power systems.
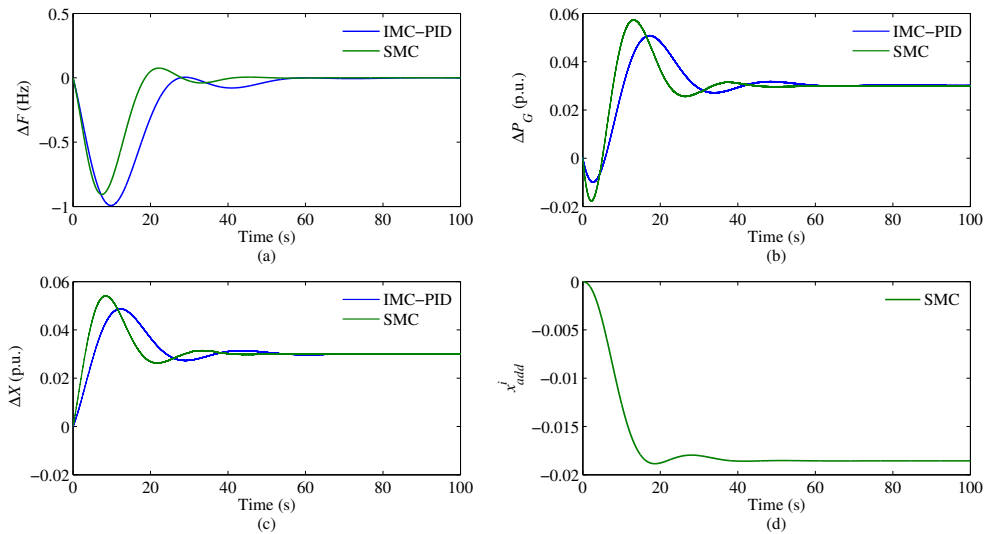
Fig. 8. Comparison of the simulation results under the isolated mode. **a**. *Frequency deviation* ΔF *;* **b**. *Power-output deviation* ΔP_G*;* **c**. *Valve-position deviation* ΔX*;* **d**. *Additional state* x^i_{add}*.*

4.3 Robustness Test

The simulation results in Figs. 8 and 9 are conducted for the nominal isolated and grid-connected system dynamics. No matter what operating mode the micro hydro plant is under, the exact values of the system parameters actually belong to a certain interval owning to the uncertainties of load in the control area and water head of the micro hydro power plant. To test the robustness of the presented method, we assume the variation is not beyond 20% so that the following parameter variation is taken into accounts, $K_p \in [40, 60]$, $T_p \in [51.71, 77.57]$ and $T_w \in [3.2, 4.8]$. Under any mode, the controller for the robustness test remains the same as the one tuned for the nominal power system dynamics. The same step load disturbance of magnitude 3% is applied at $t = 0$ for the two extreme cases.

The responses for the isolated and grid-connected modes are shown in Figs. 10 and 11, respectively. Although the control system under any mode always keeps stable in the two figures, the system performance is actually different. Under the isolated mode, the control system is sensitive for the parameter variation above the nominal system, but the aviation below the nominal will lead to a better performance. Under the grid-connected mode, the control system is not very sensitive for the parameter variation and the control performance tends to keep the same. It is clear that LFC controller and operating mode are related to the control system performance. The reason that we consider the 20% variation is that the system dynamics in Section 2 is gotten by small signal analysis. The 20% parameter variation is big enough to cover the range of the

small signal analysis. More variation is beyond the paper's scope because it may change the system dynamics.

5 CONCLUSIONS

This paper has addressed the scheme of reduced-order sliding mode control for LFC of micro hydro power plants. The LFC model of a micro hydropower plant usually include the following components, i.e., turbine & its feeding penstock, valve & its servomotor, generator & power system, and tie line. The plant usually has two operating modes, i.e., isolated mode and grid-connected mode. Under each mode, the mathematic model of each component is built up in the form of transfer function at first, and then they are interconnected with each other to formulate a block diagram of the LFC problem.

The designed controller is a model-based state feedback controller, but the number of measurable states in the block diagram is less than the system order. To attack the issue, the method of order reduction is employed. The controller under each operating mode is deduced from the order-reduced LFC model. To guarantee the controller can stabilize the original LFC model, a sufficient condition is proven in light of small gain theory. In practice, the presented control scheme is applied to a micro hydro power plant under the two modes. The robustness of the control scheme is also discussed. The simulation results show that the reduced-order SMC approach is with the better performance than the IMC-PID control approach.
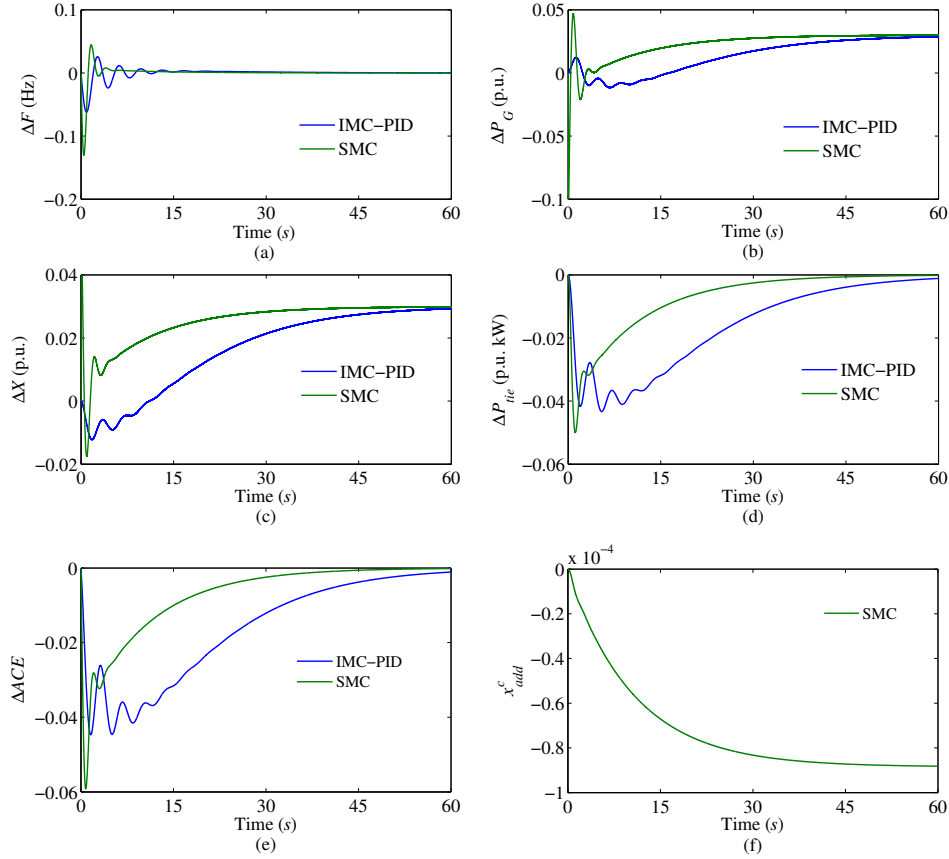
Fig. 9. Performance comparison of the simulation results under the grid-connected mode. **a**. *Frequency deviation* ΔF ; **b**. *Power-output deviation* ΔP_G; **c**. *Valve-position deviation* ΔX; **d**. *Net power* ΔP_{tie}; **e**. *Area control error* ΔACE; **f**. *Additional state* x_{add}^c.

APPENDIX

$$\Gamma = \frac{1}{T_e + T_m}$$

$$\mathbb{A}_i = \begin{bmatrix} -\dfrac{1}{T_p} & \dfrac{K_p}{T_p} & 0 & 0 \\ \dfrac{2\Gamma}{R} & -\dfrac{2}{T_w} & \dfrac{2}{T_w}+2\Gamma & 2\Gamma \\ -\dfrac{\Gamma}{R} & 0 & -\Gamma & -\Gamma \\ K_E^i & 0 & 0 & 0 \end{bmatrix}$$

$$\mathbb{B}_i = [0 \; -2\Gamma \; \Gamma \; 0]^T \quad \mathbb{C}_i = [1 \; 0 \; 0 \; 0]^T$$

$$\mathbb{F}_i = [-\frac{K_p}{T_p} \; 0 \; 0 \; 0]^T$$

$$\mathbb{A}_c = \begin{bmatrix} -\dfrac{1}{T_p} & \dfrac{K_p}{T_p} & 0 & \dfrac{K_p}{T_p} & 0 \\ \dfrac{2\Gamma}{R} & -\dfrac{2}{T_w} & \dfrac{2}{T_w}+2\Gamma & 0 & 2\Gamma \\ -\dfrac{\Gamma}{R} & 0 & -\Gamma & 0 & -\Gamma \\ 2\pi T_s & 0 & 0 & 0 & 0 \\ K_E^c\beta & 0 & 0 & K_E^c & 0 \end{bmatrix}$$

$$\mathbb{B}_c = [0 \; -2\Gamma \; \Gamma \; 0 \; 0]^T \quad \mathbb{C}_c = [\beta \; 0 \; 0 \; 1 \; 0]^T$$

$$\mathbb{F}_c = [-K_p/T_p \; 0 \; 0 \; 0 \; 0]^T$$

ACKNOWLEDGMENT

REFERENCES

[1] C.P. Ion, C. Marinescu, "Stand-alone micro-hydro power plant with induction generator supplying single phase loads," *Journal of Renewable and Sustainable Energy*, vol. 5, no. 1, pp. 1211-1216, 2013.
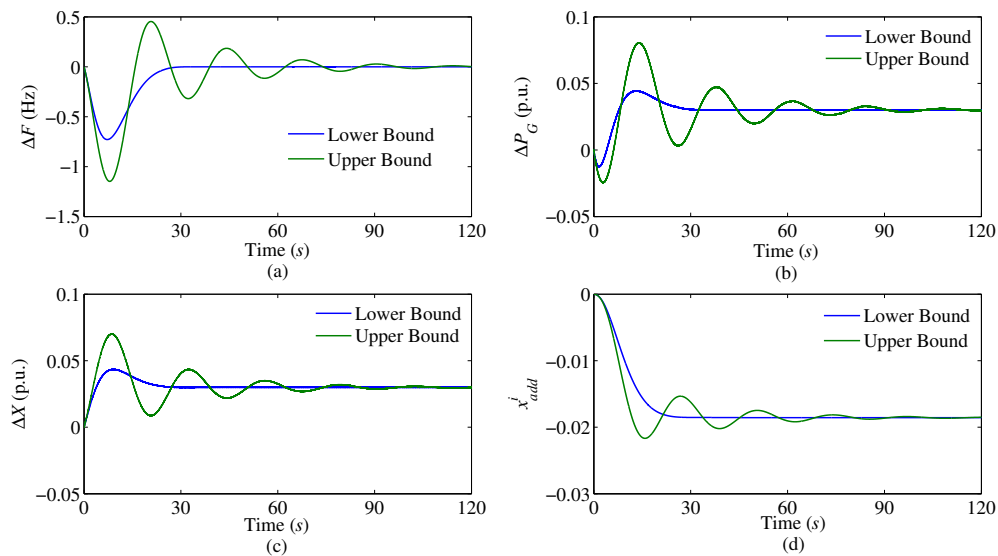
Fig. 10. Simulation results of robustness test under the isolated mode. **a.** *Frequency deviation* ΔF *;* **b.** *Power-output deviation* ΔP_G*;* **c.** *Valve-position deviation* ΔX*;* **d.** *Additional state* x^i_{add}*.*

[2] C.P. Ion, C. Marinescu, "Autonomous micro hydro power plant with induction generator," *Renewable Energy*, vol. 36, no. 8, pp. 2259-2267, 2011.

[3] K.A. Hameed, S. Palani, "Robust design of power system stabilizer using harmony search algorithm," *Automatika*, vol. 55, no. 2, pp. 162-169, 2014.

[4] O. Kuljaca, K. Horvat, B. Borovic, "Design of adaptive neural network controller for thermal power system frequency control," *Automatika*, vol. 52, no. 4, pp. 319-328, 2011.

[5] A.A. Zamani, E. Bijami, F. Sheikholeslam, B. Jafrasteh, "Optimal fuzzy load frequency controller with simultaneous auto-tuned membership functions and fuzzy control rules," *Turkish Journal of Electrical Engineering & Computer Sciences*, vol. 22, no. 1, pp.66-86, 2014.

[6] J.L. Marquez, M.G. Molina, J.M. Pacas, "Dynamic modeling, simulation and control design of an advanced microhydro power plant for distributed generation applications," *International Journal of Hydrogen Energy*, vol. 35, no. 11, pp. 5772-5777, 2010.

[7] I. Salhi, S. Doubabi, N. Essounbouli, A. Hamzaoui, "Application of multi-model control with fuzzy switching to a micro hydro-electrical power plant," *Renewable Energy*, vol. 35, no. 9, pp. 2071-2079, 2010.

[8] M. Hanmandlu, H. Goyal, "Proposing a new advanced control technique for micro hydro power plants," *International Journal of Electrical Power & Energy Systems*, vol. 20, no. 4,pp. 272-282, 2008.

[9] S. Doolla, T.S. Bhatti, R.C. Bansal, "Load frequency control of an isolated small hydro power plant using multi-pipe scheme," *Electric Power Components and Systems*, vol. 39, no. 1, pp. 46-63, 2011.

[10] B. Singh, V. Rajagopal, "Neural-Network-Based integrated electronic load controller for isolated asynchronous generators in small hydro generation," *IEEE Transactions on Industrial Electronics*, vol. 58, no. 9, pp. 4264-4274, 2011.

[11] L. Belhadji, S. Bacha, I. Munteanu, A. Rumeau, D. Roye, "Adaptive MPPT applied to variable-speed microhydropower plant," *IEEE Transactions on Energy Conversion*, vol. 28, no. 1, pp. 34-43, 2013.

[12] E. Özbay, M.T. Gençglu, "Load frequency control for small hydro power plants using adaptive fuzzy controller," in Proceedings of IEEE 2010 International Conference on Systems, Man and Cybernetics, (Istanbul, Turkey), pp. 4217-4223, Oct. 2010.

[13] H. Mohamad, H. Mokhlis, A. Abu Bakar, H.W. Ping, "A review on islanding operation and control for distribution network connected with small hydro power plant," *Renewable and Sustainable Energy Reviews*, vol. 15, no. 8, pp. 3952-3962, 2011.

[14] V.I. Utkin, *Sliding Modes in Control and Optimization (2nd ed)*. Berlin, Germany: Springer-Verlag, 1992.

[15] M. Dybkowski, T. Orlowska-Kowalska, G. Tarchala, "Sensorless traction drive system with sliding mode and MRAS(CC) estimators using direct torque control," *Automatika*, vol. 54, no. 3, pp. 329-336, 2013.

[16] D. Liu, M.G. Li, "Adaptive wavelet neural network backstepping sliding mode tracking control for PMSM drive system," *Automatika*, vol. 55, no. 4, pp. 405-415, 2014.

[17] L. Cheng, Z. Hou, M. Tan, "A mean square consensus protocol for linear multi-agent systems with communication noises and fixed topologies," *IEEE Transactions on Automatic Control*, vol. 59, no. 1, pp. 261–267, 2014.
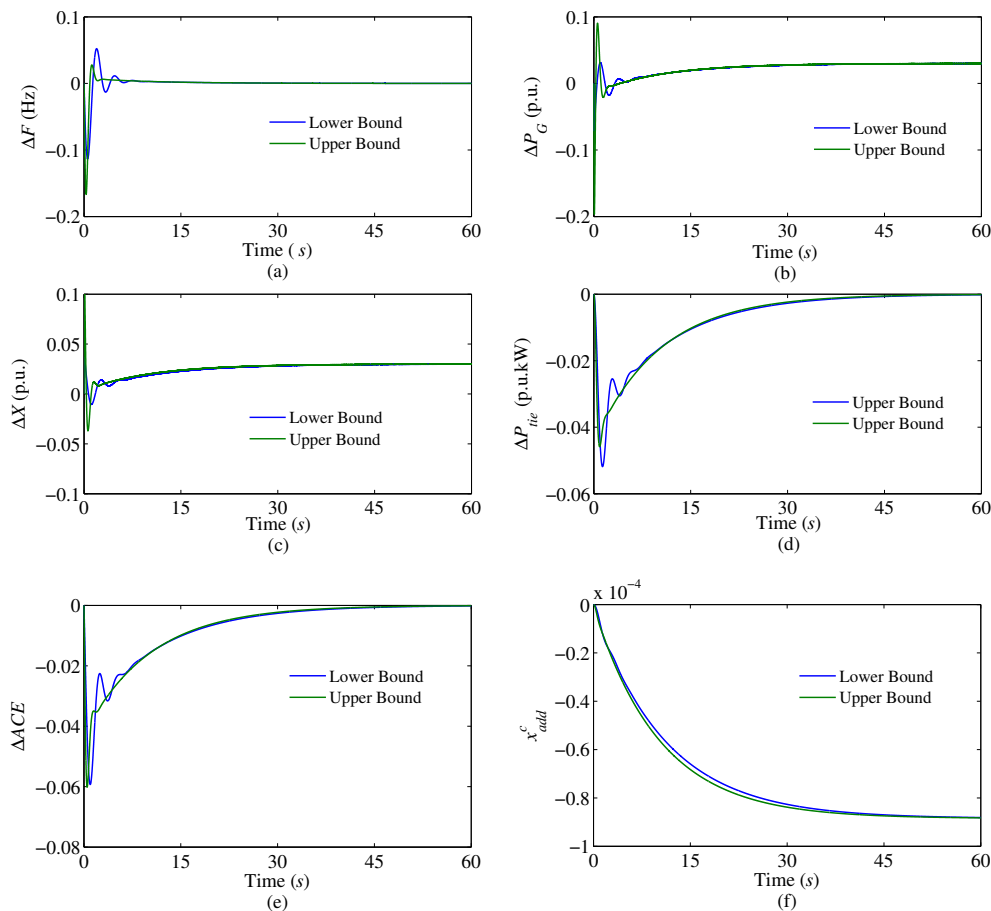
*Fig. 11. Simulation results of robustness test under the grid-connected mode. **a**. Frequency deviation ΔF ; **b**. Power-output deviation ΔP_G; **c**. Valve-position deviation ΔX; **d**. Net power ΔP_{tie}; **e**. Area control error ΔACE; **f**. Additional state x^c_{add}.*

[18] L. Cheng, Y. Wang, Z. Hou, M. Tan, Z. Cao, "Sampled-data based average consensus of second-order integral multi-agent systems: switching topologies and communication noises," *Automatica*, vol. 49, no. 5, pp. 1458–1464, 2013.

[19] A. Zargari, R. Hooshmand, M. Ataei, "A new control system design for a small hydro-power plant based on particle swarm optimization-fuzzy sliding mode controller with Kalman estimator," *Transactions of the Institute of Measurement and Control*, vol.34, no. 4, pp. 388-400, 2012.

[20] D. Qian, J. Yi, X. Liu, "Design of reduced order sliding mode governor for hydro-turbines," In Proceedings of 2011 American Control Conference, (San Francisco, CA), pp.5073-5078, June 29 -July 1 2011.

[21] X. Ding, A. Sinha, "Sliding mode/H$_\infty$ control of a hydro-power plant," In Proceedings of 2011 American Control Conference, (San Francisco, CA), pp. 5201-5206, June 29 -July 1 2011.

[22] K. Vrdoljak, N. Peric, I. Petrovic, "Applying optimal sliding mode based load-frequency control in power systems

with controllable hydro power plants," *Automatika*, vol. 51, no. 1, pp. 3-18, 2010.

[23] K. Vrdoljak, N. Peric, I. Petrovic, "Sliding mode based load-frequency control in power systems," *Electric Power Systems Research*, vol. 80, no. 5, pp. 514-527, 2010.

[24] R. Hooshmand, M. Ataei, A. Zargari, "A new fuzzy sliding mode controller for load frequency control of large hydropower plant using particle swarm optimization algorithm and Kalman estimator," *European Transactions on Electrical Power*, vol. 22, no. 6, pp. 812-830, 2012.

[25] S.C. Tripathy, V. Bhardwaj, "Automatic generation control of a small hydro-turbine driven generator," *Energy Conversion and Management*, vol. 37, no. 11, pp. 1635-1645, 1996.

[26] S. Saxena, Y.V. Hote, "Load frequency control in power systems via internal model control scheme and model-order reduction," *IEEE Transactions on Power Systems*, vol. 28, no. 3, pp. 2749-2757, 2013.

[27] Z.M. Al-Hamouz, H.N. Al-Duwaish, "A new load frequency variable structure controller using genetic algorithms", *Electric Power Systems Research*, vol. 55, no. 1, pp. 1-6, 2000.

[28] W. Tan, Z. Xu, "Robust analysis and design of load frequency controller for power systems," *Electric Power Systems Research*, vol. 79, no. 5, pp. 846-853, 2009.

[29] H.K. Khalil, *Nonlinear Systems (3rd ed)*. New Jersey, NY, USA: Prentice Hall, 2002.

[30] D.W. Qian, D.B. Zhao, J.Q. Yi, X.J. Liu, "Neural sliding-mode load frequency controller design of power systems," *Neural Computing & Applications*, vol. 22, no. 2, pp. 279-286, 2013

[31] W. Tan, Unified tuning of PID load frequency controller for power systems via IMC, *IEEE Transactions on Power Systems*, vol. 25, no. 1, pp.341-350, 2010.

Dianwei Qian received the B.E. degree from the Hohai University, Nanjing, China, in 2003. He received the M.E. degree from Northeastern University, Shenyang, China, and the Ph.D. degree from the Institute of Automation, Chinese Academy of Sciences, Beijing, China, in 2005 and 2008, respectively. Currently, he is an associate professor with the School of Control and Computer Engineering, North China Electric Power University, Beijing, China. His research interests are in the theory and application of intelligent and nonlinear control.

Shiwen Tong received the B.E. degree in chemical engineering from the University of Petroleum (East China), Shandong, China, in 1999, the M.E. degree in control theory and control engineering from the University of Petroleum (Beijing), Beijng, in 2003, and the Ph.D. degree from the Institute of Automation, Chinese Academy of Sciences, Beijing, in 2008. He is currently on staff with the College of Automation at Beijing Union University. His research interests include intelligent control, networked control, proton exchange membrane fuel cells, and their industrial applications.

Xiangjie Liu received the Ph.D. degree in electrical and electronic engineering from the Research Center of Automation, Northeastern University, Shenyang, China, in 1997. He subsequently held a postdoctoral position with the China Electric Power Research Institute (CEPRI), Beijing, China, until 1999. He has been an Associate Professor in CEPRI since 1999. He was a Research Associate with the University of Hong Kong, and a Professor with National University of Mexico. He is now a Professor with the School of Control and Computer Engineering, North China Electric Power University, Beijing, China. His current research areas include fuzzy control, neural networks, model predictive control with their applications in industrial processes.

AUTHORS' ADDRESSES
Dianwei Qian, Ph.D.
Prof. Xiangjiu Liu, Ph.D.
School of Control and Computer Engineering,
North China Electric Power University,
No. 2 Beinong Road, Changping District, Beijing, P.R. China
e-mail: dianwei.qian@ncepu.edu.cn, ia_ac@163.com

Shiwen Tong, Ph.D.
College of Automation,
Beijing Union University,
No.97 Beisihuan Donglu, Chaoyang District, Beijing 100101,
P.R. China
e-mail: shiwen.tong@buu.edu.cn